Accuracy Assessment of InSAR derived Input maps for Landslide Susceptibility Analysis: A Case study from the Swiss Alps

Lalan P. Singh [a,] , **C. J. van Westen** [a], **P. K. Champati Ray** [b], **P. Pasquali** [c]

[a] *ESA Department, International Institute for Geo-Information Science and Earth Observation, Enschede, The Netherlands*
[b] *Indian Institute of Remote Sensing, , Dehradun, India*
[c] *Sarmap, Cascine de Barico, Purasca, Switzerland*

ABSTRACT

In recent years SAR interferometry has become a widely used technique for measuring topography and displacement at the earth's surface. Both these capabilities are highly relevant for landslide susceptibility studies. Although there are many problems that make the use of SAR interferometry less suitable for landslide inventory mapping, the generation of input maps for landslide susceptibility assessment looks very promising.The present work attempts to assess the usefulness and limitations of this technique based on a case study in the Swiss Alps. Input maps were generated from ERS repeat pass data using SAR interferometry. A land cover map has been generated by image classification of multi-temporal intensity images. Slope, aspect, relief and slope form are derived from an InSAR DEM. These maps have been used to generate landslide and rockfall susceptibility maps, which correlate fairly well with the existing landslide inventory map. However, the comparison of InSAR DEM with the Swisstopo DEM (DHM25), indicates significant errors in the absolute height and slope anlges derived from InSAR, especially along the ridges and in the valleys. Correct estimation of slope is crucial for landslide susceptibility zonation. Since maximum deviation in the height is confined along the ridges and valleys it indicates that these errors are caused by low coherence mostly due to layover and shadow effects. Visual comparision of stereo simulations created from hill shading maps and corresponding DEMs demonstrate that topographic details have been lost in the InSAR-derived DEM. It is concluded that InSAR derived input maps are not ideal for landslide susceptibility assessment, but could be used if more accurate data is lacking.

1. INTRODUCTION

SAR interferometry (InSAR) is gaining increasing importance as a technique for rapid and accurate topographic data collection. Digital Elevation Models (DEM) produced from this technique are becoming available to general science and operational communities, for example the general DEMs produced by the SRTM mission (Balmer, 2003). In recent years this technique has been used to monitor and measure landslide movements (Fruneau, *et al.*, 1996; Rott, *et al.*, 1999 and Vietmeier *et al.*, 1999). Attempts are being made to integrate radar Interferograms, field measurements, and other remote sensing data of landslides to obtain calibrated interferograms for getting useful information with regard to the landslide monitoring (e.g. *Bulmer et al.,* 2001). Also, a number of InSAR systems are operational or in the planning and implementation stages and therefore it is important to understand the accuracy and limitations of the technique for different applications. In this paper we examine the usefulness of InSAR DEM and intensity images generated from ERS repeat pass data for landslide susceptibility assessment. The findings presented in this paper are based on a case study in the Swiss Alps. The area is situated in south Switzerland, in the cantons of Fribourg and Bern (See Figure1). The landscape in the region is marked by several glacial, hydrological and gravitational processes such as landslides and rockslides (Monbaron, *et al.*, 2002). Debris flows, rockfalls and snow avalanches are also quite predominant in the area.

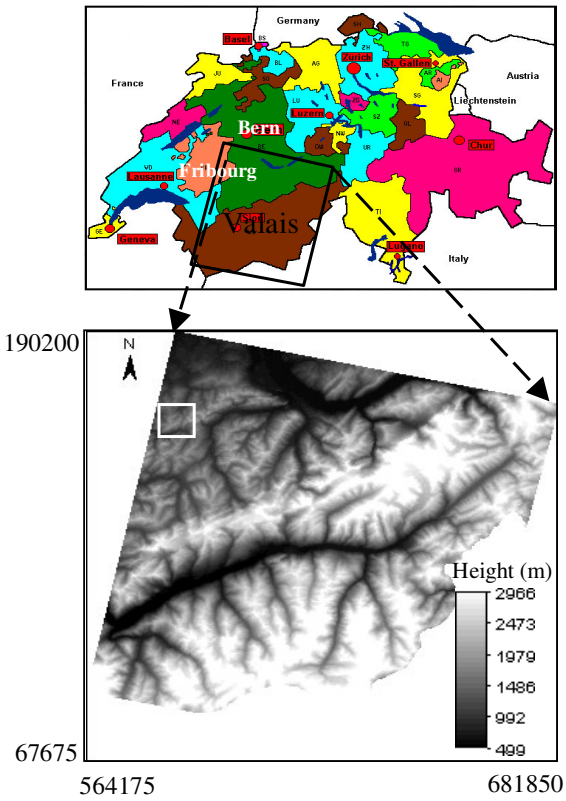

Figure 1: Study area shown in the white square an InSAR-derived DEM.

2. INPUT MAP GENERATION FOR LANDSLIDE SUSCEPTIBILITY ASSESSMENT

ERS tandem data of 7 & 8 November 1995, 22 & 23 October 1996 and ERS – 2 data of 5 April, 19 July, and 27 September 2000 have been used to generate input maps for landslide susceptibility assessment, such as land cover, slope, aspect, slope form and relief. The data processing was done by Sarscape software (Sarmap, 2002). In this section the procedure is explained.

Extraction of Land Cover Map by Image Classification of Multi temporal intensity Images

The different brightness levels in the Radar intensity images help to differentiate the terrain features. If multi temporal intensity images are available valuable information on land cover may be extracted as the brightness characteristics change depending on the type of land cover units. For the present study the intensity images were generated from the three available ERS Single Look Complex (SLCs) data of 5 April, 19 July and 27 September 2000 using a focusing and multilooking operation of SARscape software. All the intensity images were then co-registered and filtered for speckle removal using a time series filter. By applying this filter the full spatial resolution of the imagery is retained while there is a significant increase in the signal to noise ratio (SNR) (De Grandi et al., 1997). In this way, homogenous regions are optimally filtered while structural features are retained. These images were then geocoded and a False Colour Composite (FCC) was generated which shows wide variability in terms of radar response of the region. In other words, it was possible to discriminate different colour classes in the FCC. Training sites were selected from all the classes and Jeffries-Matusita distance measures (Chips, 2002) were implemented for determining separability of the classes and it was observed that most of the classes were statistically separable. A Maximum

Likelihood classification was performed with standard deviation of 2 for the variability of each class. The resulting land cover map is shown in Figure 2. The result shows good classification accuracy for all classes, however with the following exceptions.

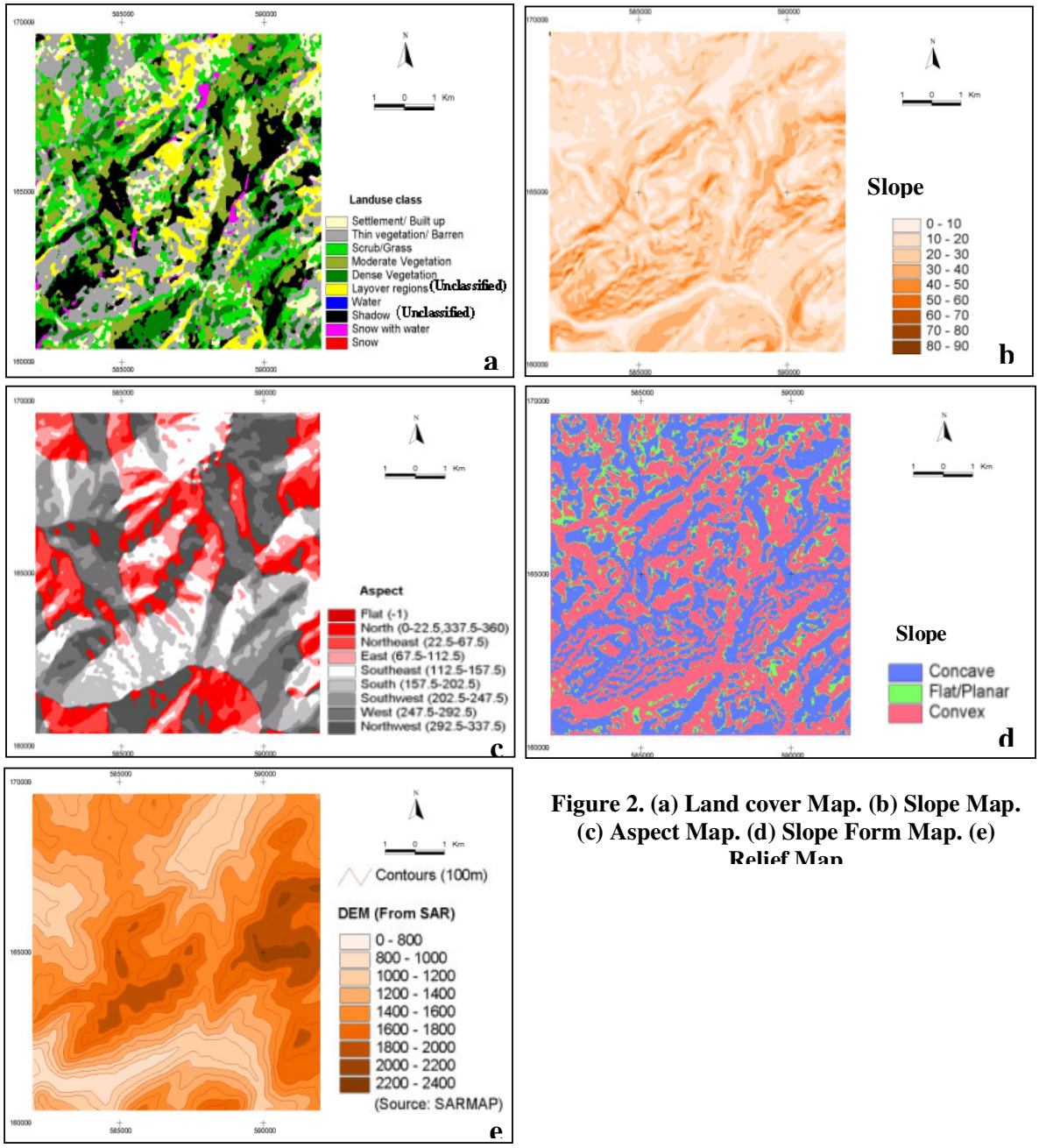

Figure 2. (a) Land cover Map. (b) Slope Map. (c) Aspect Map. (d) Slope Form Map. (e) Relief Map

1. Snow with melt water was misclassified as lakewater, which could easily be maked out with the help of a reference DEM and topomap.

2. Similarly some areas in high altitude were wrongly classified as settlement areas due to inseperability of pixels representing snow from those of settlement. However, this misclassification could be undone by comparison with DEM. At some places, the grassland

and river classes were mixed up due to the pixel impurity in adjoining areas of the river. However this was resolved with priori information in selected parts.

3. About 24% of the land cover map could not be classified due to shadow (16%) and layover (8%), and therefore these areas have been indicated as unclassified.

Generation of a DEM from InSAR

The InSAR DEM used for the present study was produced from ERS tandem data of 7 & 8 November 1995 and 22 & 23 October 1996. . A combination of ascending and descending mode data were used as this combination is essential for covering all slopes in the terrain (Pasquali, *et al.,* 1994). It is because the areas affected by foreshortening and layover in one image (e. g. ascending mode) are well covered (if not in shadow) in the other image (e. g. descending mode). The InSAR processing involved: coregistration of the two tandem data, calculation of the interferometric phase and coherence, phase unwrapping and computation of the height. Since the phase unwrapping is the most crucial part of InSAR processing involving reconstruction of phase to extract height information, any error committed at this stage affects the quality of the DEM. Various algorithms exist for unwrapping but no single one is sufficient. To overcome this problem a hybrid approach is implemented in the SARscape software which is based on the fusion of a region growing and an iteratively working 2-D least square phase unwrapping algorithm (Reigber and Moreira, 1997). By the mutual support of the two algorithms it was possible to combine the advantages of both and to eliminate the errors, which might have occurred if working with both methods independently.

The unwrapped phase was converted into x, y, z Cartesian coordinates by employing range and Doppler approach using slant range, the doppler and the interferometric equations (Holecz, et al., 1998). The phase to height conversion implemented in the SARscape software is based on a rigorous approach and does not require a priori known DEM for geocoding of SAR-derived DEM (Holecz, personal commun.). This approach is based on a fully three-dimensional model that connects the image space to object space. It uses observation equations that connect the image space (azimuth, slant range and interferometric phase) to the object space (Cartesian system) (Crosetto, 2002). The procedure works pixel-wise and thus requires precise orbit knowledge of the two satellites (master and slave). However, the accuracy of the satellite orbits is usually not sufficient to achieve an accurate DEM geocoding and therefore an InSAR geometry calibration with points of known height are needed. This was done by selecting GCPs from the GTOPO-30 DEM of USGS and converting it into slant range geometry. The points were selected from the part of the unwrapped image where coherence is good (more than 0.3 is preferred), where there are no problems in the unwrapping (e.g. not in areas that have a phase value very different from the surrounding region or discontinuities). The DEM was generated using a coherence threshold of 0.25. Interpolation was applied as the 3D points generated from interferometric phases are unevenly distributed because of two reasons (1) the slant rang nature of SAR data makes the terrain sampling very irregular, (2) the phase of many interferogram pixels cannot be unwrapped: such pixels do not contribute to the grid generation, i.e. they result in “holes” in the grid (Crosetto, 2002). The grid size of the DEM is 25 m.

Input map generation from InSAR DEM

Several parameter maps for landslide susceptibility assessment, were generated from the DEM,: relief, slope, aspect and slope form. These fundamental topographical parameter maps were considered important for susceptibility analysis as they have direct or indirect relationship with the slope stability of the region. For deriving these parameters the InSAR DEM was imported to ILWIS 3.11 GIS software and using various modeling functionalities the maps were generated and each of them were reclassified (See Figure 2).

3. STATISTICAL LANDSLIDE SUSCEPTIBILITY ASSESSMENT USING InSAR - DERIVED PARAMETER MAPS

The input maps generated from InSAR were used in a GIS environment and two separate susceptibility maps for the two most prominent types of landslides in the area (i. e., debris slides / flow slides and rock fall) were generated using weights of evidence method (Bonham-Carter, 1994). Rock fall and shallow debris slides were treated separately as these are two completely different phenomena governed by different terrain conditions. The landslide inventory map provided by the Swiss Federal Office for Water and Geology (FOWG) was used to develop the model and also for the validation of the results. For validation of the two susceptibility maps two separate maps, showing the rock falls (See Figure 3a) and the shallow landslides (See Figure.3b) were generated by reclassifying the units in the landslide inventory map of FOWG. The two susceptibility maps are described in the following sections.

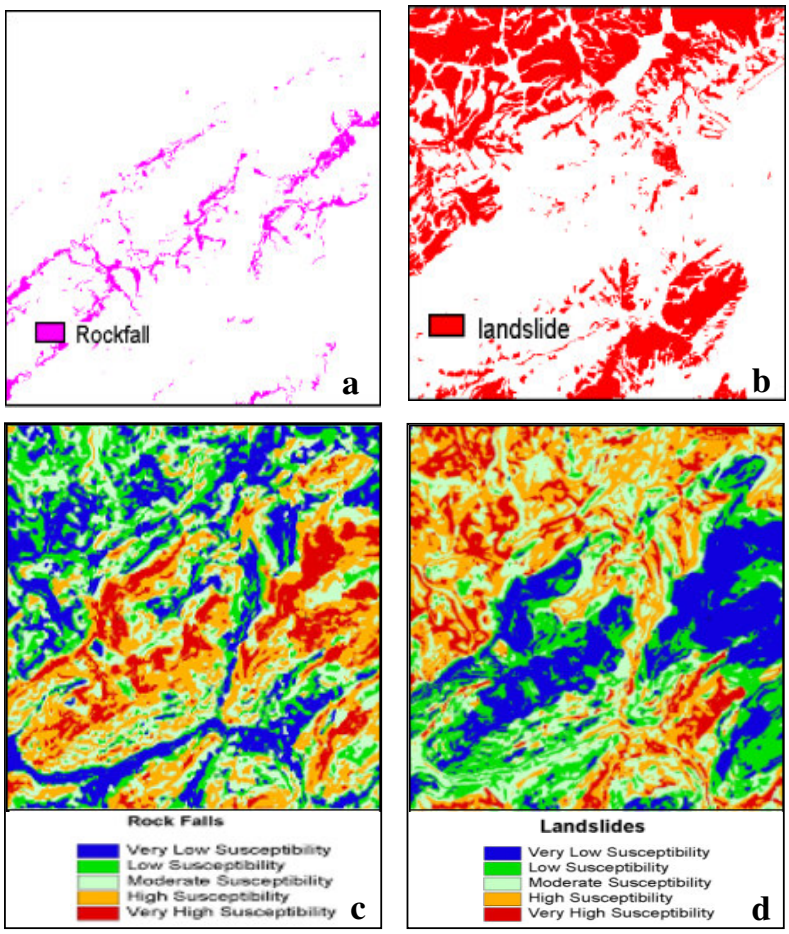

Figure. 3. (a) Rockfall Map. (b) Landslide Map. (c) Rockfall Susceptibility Map. (d) Landslide Susceptibility Map

Rock fall susceptibility map

The rockfall inventory map was combined with the parameter maps (e. g., land cover, slope, aspect, slope form and relief maps) through map overlaying in GIS, followed by the calculation of weights indicating the statistical relation of each class of the parameter maps with the rockfall phenomena. In the land cover map (Figure 2a), it was observed that the unclassified areas such as shadow zone and snow cover regions, which are often associated with high altitude regions in the study area, show positive relation with rock falls. In the slope

map (Figure 2b), the slopes falling in slope classes greater than 30^0 angles bear a positive relationship with the occurrence of rock fall. In the slope aspect map (Figure 2c), it was observed that the north and northwest oriented slope classes have a positive correlation perhaps due to the fact that they are in shadow most of the time and experience more freezing activity leading to mechanical disintegration of rocks. In the slope form map (Figure 2d), mostly the convex slopes are associated with rock fall. In the relief class map (Figure 2d) the classes with an altitude of more than 1600 m are associated with rock falls.. After analyzing the final weights for all the classes in different parameter maps, the rock fall susceptibility map was generated and classified into qualitative susceptibility classes (Figure 3c).

The rock fall susceptibility map was validated with the rock fall map (Figure 3a) using the weights of evidence method (Van Westen, 1993). The susceptibility classes show an overall good statistical validation, with negative weight values falling in very low susceptibility class and gradually becoming positive as one moves towards the higher susceptibility classes (Table 1). However, one exception is the moderate class, which ideally should show near zero weight value but it shows negative weight and 6.19% of total rockfalls in the area fall in this class.

Table 1. Validation of rockfall susceptibility zonation map with respect to rock falls using a statistical approach (Weights of Evidence method)

Susceptibility Class	WPLUS	WMIN	WFINAL	Rockfall (%)
Very Low	-3.0915	0.2265	-3.5141	0.96
Low	-2.6427	0.2165	-3.0553	1.47
Moderate	-1.4296	0.2352	-1.8609	6.19
High	0.4574	-0.2080	0.4689	38.59
Very High	1.8812	-0.6670	2.3518	52.79

Shallow landslide susceptibility map

The statistical relationship of the landslide map with the parameter maps supports the assumption that shallow landslides occur under a different geoenvironmental setting, than rock falls in the region. In the land cover map, the classes such as grassland, dense vegetation and thinly vegetated areas, which mostly occur on gentle slopes of the hills, show positive relation with the occurrence of landslides. In contrast, the classes having positive weights for rock falls show a negative relation for landslides. The weights for the slope aspect classes indicate that southwestern and western slopes experience more of shallow slides. The slope curvature map indicates that concave slopes are mostly associated with landslides. In the relief map, the 1200-1400m class and adjoining relief classes show positive relationship with landslides. The landslide susceptibility map was generated by combining the weights of the parameter maps , and this map was classified using cumulative cut off at 20%, 40%, 65%, and 85% (Figure 3d). The classified map shows a good correlation with actual landslides in the region (Figure 3b & Table 2).

4. ACCURACY ASSESSMENT OF THE INSAR DEM

The accuracy assessment of InSAR DEM products was attempted with a view to have some insight into the reliability of susceptibility maps generated from these products. A comparison of a part of the InSAR DEM used for deriving input maps for susceptibility assessment, was made with the DHM25 matrix model produced by Swisstopo, Switzerland (Swisstopo, 2002). The DHM25 matrix model was derived by applying triangulation network interpolation to the basis model, which was extracted from the National Map (vectorized contours) of 1:25 000. The DHM25 has the same coordinate system and grid size as InSAR DEM (Swiss Coordinate System and a grid size of 25 m). The average accuracy of DHM25 with respect to

photogrammetrically determined control points is about 3 m (Swisstopo, 2002). The error estimation was done for the absolute height as well as for slope because for landslide susceptibility assessment slope is a more important factor than the absolute height. For determining the effect of error in slope measurement on susceptibility classes the weights of evidence test was applied on the slope maps generated from the two DEMs.

Table 2. Validation of landslide susceptibility zonation map with respect to actual known landslides using a statistical approach (Weights of Evidence method)

Susceptibility Class	WPLUS	WMIN	WFINAL	Landslide %
Very Low	-2.9867	0.2921	-3.3472	1.49
Low	-1.3982	0.2215	-1.6881	6.55
Moderate	0.0782	-0.0270	0.0366	27.13
High	0.8031	-0.3410	1.0759	42.15
Very High	1.4843	-0.2140	1.6299	22.67

Error Estimation of InSAR height with respect to DHM25

For height error estimation the InSAR DEM was subtracted from DHM 25 and an absolute elevation difference map was generated and reclassified into elevation difference classes (Figure 4).

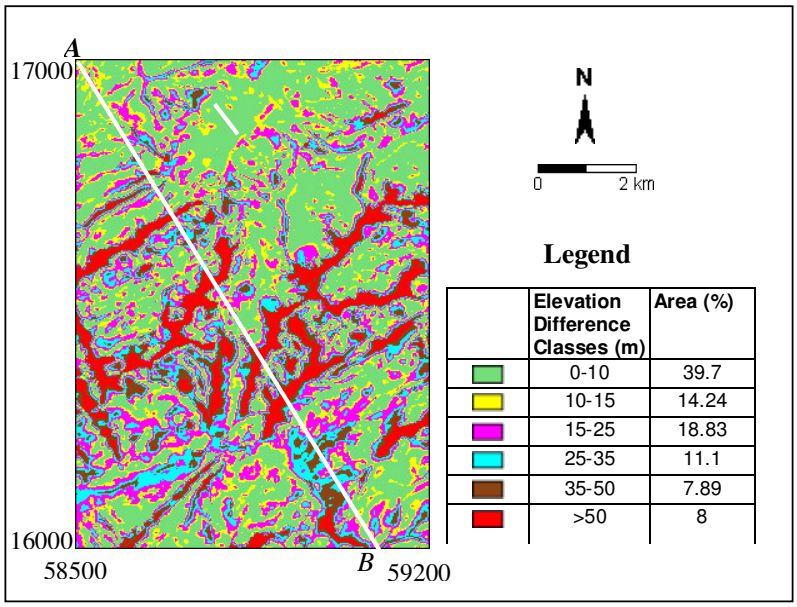

Figure 4. Elevation Difference Map (DHM25 – InSAR DEM). A - B is the line along which profile has been drawn in both the DEMs. C – C' is the line along which the scatter plot of DEM values have been made in Figure 5

As the altitude values derived from InSAR provide a geometric altitude (i.e. height above a reference ellipsoid) while the altitude from DHM25 (derived from a topographic map)is a gravimetric altitude (i.e. height above mean sea level), it is often required to transform the datum before comparing the two DEMs (Gens and van Genderen, 1996). To determine whether a datum transformation is required prior to comparing the two DEMs a scatter plot was made of the DEM values along a selected line from the part of the DEMs where the elevation difference is less than 10 m. The best line fit through the values crosses the x-axis at a distance of 4 m from the origin which is more than the standard deviation (S. D. = 0.167) of the observed values of corresponding points in the two DEMs (Figure 5). This indicates that there is an offset of +- 4 m in the datum of the two DEMswhich is negligible compared to the large differences in the height measurement as seen in the absolute elevation difference map (Figure 4) Variation in height in the order of more than 50 m exists in about 8% of the map area and most of these areas are confined along the mountain ridges and valley bottoms.

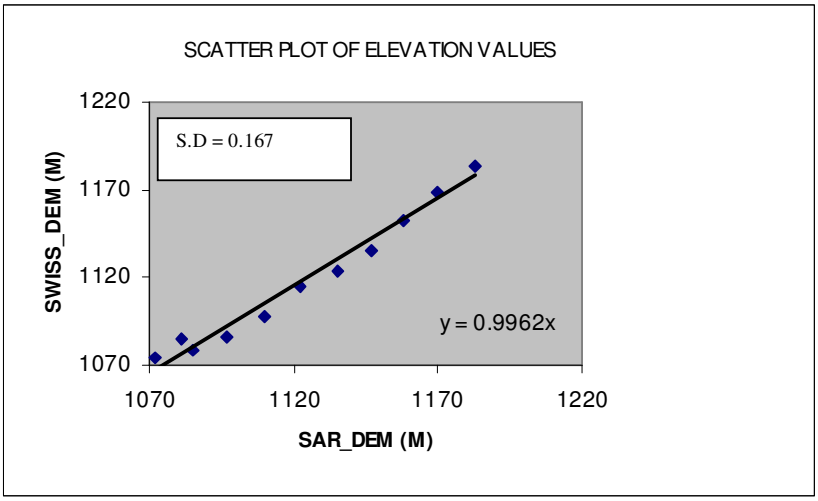

Figure 5. Scatter plot of DEM values along line C – C' in Figure 4

Error Estimation in Slope Classes

Since slope classes are more important factors for landslide susceptibility zonation as compared to absolute elevation, slope maps were generated from both the InSAR DEM and the DHM25, using the same method. The two slope maps were compared and the results are shown in Table 3.

Table 3. Area under different slope classes in DHM25-derived and InSAR-derived slope maps

Slope Class **(Degree)**	**DHM25** **Area (%)**	**InSAR DEM** **Area (%)**
<10	8.7	15.11
10--20	25.87	37.57
20--30	29	31.2
30--40	24.25	14.06
40--50	8.45	2.04
>50	3.74	0.03

From Table 3 it is evident that areas with a slope from 0^0 to 30^0 are significantly larger in the InSAR DEM derived slope map as compared to the DHM25 derived slope map. But in the steeper slopes of more than 30^0 there are smaller areas in InSAR DEM than in DHM25. A comparison of profiles drawn in each DEM across the general trend of ridges (along line A – B in Figure 4) clearly reveals the differences in height and slope angle (Figure 6).

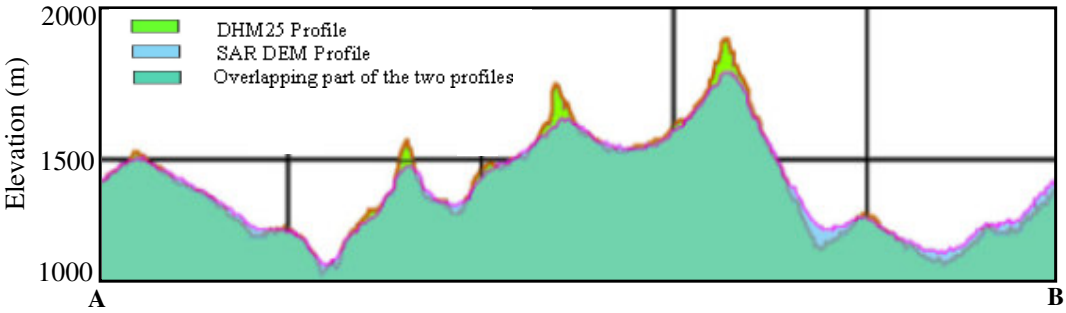

Figure 6. DHM25 and InSAR DEM profiles along line A – B of Figure 4.

It is evident that on the mountain ridges the InSAR DEM underestimates both the height and slope angles while along the valley sides it shows smaller slope angles and greater altitudes as compared to the DHM25. From these observations it can be concluded that InSAR DEM smoothens the topography. The smoothening effect of InSAR DEM is also demonstrated by the visual examination with 3-D perspective in anaglyphs created from the hill shading maps of DHM25 and InSAR DEM. The topographic details appear to be more blurred in the InSAR DEM anaglyph (Figure 7, use of red-green glasses is required for stereo-viewing). These observations are critical for susceptibility zonation as slope classes are significant factors for the occurrence of landslides. Also the $20\text{-}30^0$ slope class is critical for construction of civil structures and any overestimation of area under this class from the actual situation is detrimental.

Comparison of weights of evidence of rock fall for slope maps derived from DHM25 and InSAR DEM

The effect of the error in altitude and slope on the landslide susceptibility mapping was evaluated by calculating landslide weights for both slope maps derived from InSAR DEM and the DHM25. From the weight values of the slope classes for rock falls as shown in Table 4 two trends can be inferred: (i) In the DHM25-derived slope map only the slopes steeper than 40^0 show positive weights for occurrence of rock fall whereas in the InSAR DEM-derived slope map the positive weights are observed right from slopes of 20^0 or steeper; (ii) In the InSAR derived slope map the weight values for all the slope classes are greater than those in corresponding slope classes of DHM25. The reason for the positive weight value even in the moderate slope of $20\text{-}30^0$ in InSAR derived slope map could be due to overestimation of areas under this class. Some of
the areas, which are actually steeper, were wrongly included in the less steep classes due to the smoothening effect in the InSAR DEM as explained earlier and the positive weight of this class is due to the contribution from the more susceptible steeper areas which are incorrectly included in this slope category. From these trends of weight values, it may be concluded that the susceptibility map derived from InSAR DEM-derived input maps is more conservative as it includes more areas under positive weights for rockfall.

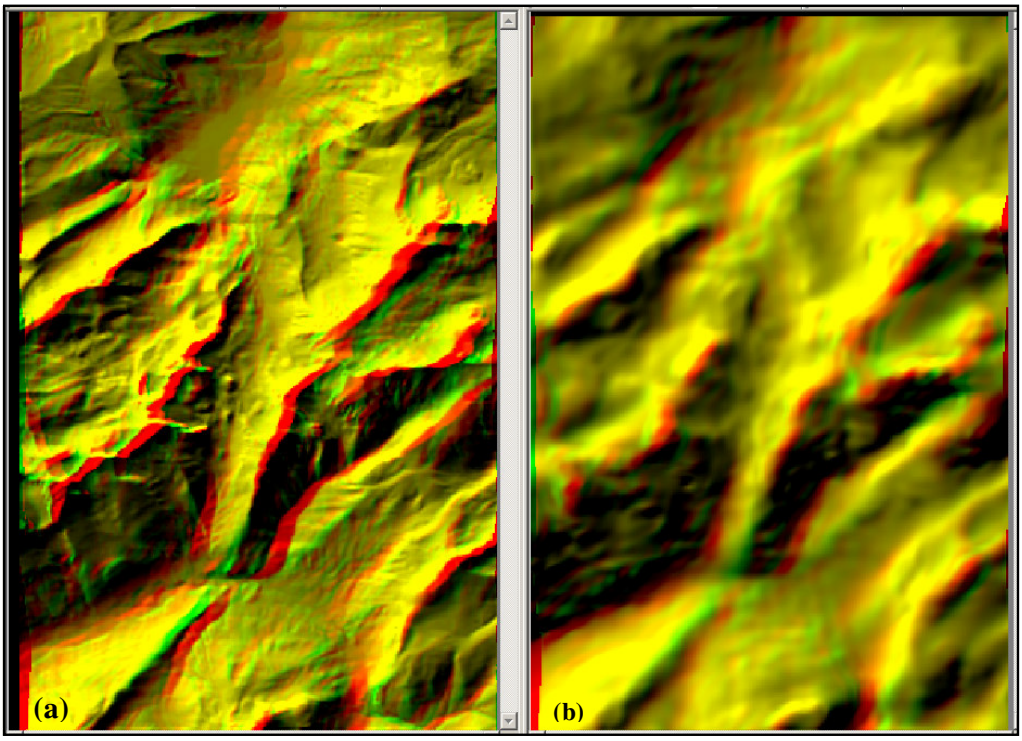

Figure 7: Anaglyphs generated from hill shadow maps of DEMs. (a) DHM25 and (b) SAR DEM

Table 4: Rockfall weight (WFINAL) values for slope and aspect classes derived from DHM25 and SAR DEM

Slope Class	DHM25	InSAR DEM
	WFINAL	WFINAL
<10	-2.782	-1.0798
10 --20	-2.8162	-1.1043
20--30	-2.139	0.1619
30--40	-0.5505	1.1604
40--50	1.6625	1.9212
>50	3.5751	4.1054

Comparison of weight of evidence of debris slides for factor maps derived from DHM25 and SAR DEM

From the weight values for debris slides as shown in Table 5 it appears that the slope classes between 10-30^0 show a positive relationship with debris slides in the DHM25 indicating that gentle to moderate slopes are more susceptible to these type of mass movement. The comparison of weight values indicates that both maps have a similar trend except for the 20-30^0 class. This class in the InSAR-derived slope map shows a negative relationship with the occurrence of landslides and thus contradicts with the weight value of DHM25 for the same slope class. Earlier it has been observed that for rock fall the same class in InSAR derived slope shows a positive weight. This observation further confirms that the majority of pixels in 20-30^0 slope class of InSAR derived slopes are in reality steeper slopes, which are less susceptible to debris slide.

Table 5: Debris slide weight (WFINAL) values for slope and aspect classes derived from DHM25 and SAR DEM

	DHM25	**InSAR DEM**
Slope Class	WFINAL	WFINAL
<10	-0.54134	-0.29111
10 --20	0.940195	0.774819
20--30	0.272189	-0.37411
30--40	-0.92901	-1.63501
40--50	-1.95066	-3.74108
>50	-3.98398	-2.25563

5. Discussion and conclusions

Important terrain parameter layers for landslide susceptibility analysis can be extracted from InSAR DEM and through image classification of different combinations (False Colour Composites) of multi temporal intensity images. The landslide susceptibility maps generated from the InSAR-derived input maps show good correlation with the original landslide inventory map. However, the accuracy of individual parameter map classes is not always satisfactory. For example, the water class in the land cover map shows a positive weight value for rockfall susceptibility, which is highly unlikely. The reason for this could be ascribed to the error in classification which might have arisen due to the problem of mixed pixels from other classes, especially the "snow with melt water" class. The problem of mixed pixels can be avoided if the SAR images acquired during the summer period are used for land cover classification. It is because during the summer period the area will not be covered by snow and hence the backscatter characteristics will be different from when the same terrain is covered by snow. The comparison of the InSAR DEM with a DEM derived from a topographical map (DHM25) gives differences in height in the order of more than 50 m in high relief areas and in shadow zones in the valleys. The mean value of the difference is 20 m with standard deviation of 21.5 m. Even though the altitude values derived from InSAR and DHM25 differ from each other because the former provides a geometric altitude (i. e. height above a reference ellipsoid) while the latter provides a gravimetric altitude (i. e. height above mean sea level) (Gens and van Genderen, 1996), the deviation observed in the present case is too high to be caused only due to the reason stated. The comparision of profiles of InSAR DEM and DHM25 indicates that the InSAR underestimates the height at mountain tops while overestimating the lowest parts of the valleys. Platschorre (1997) states that this deviation is

caused by the least square phase unwrapping. But in the present case a more sophisticated algorithm, which uses the fusion of a region growing and least square fit, has been applied and therefore the existence of these large errors on critical part of the slopes raise limitations of the InSAR-derived products for landslide susceptibility studies. It is because the slope class is a critical parameter for slope stability and any erroneous estimation of slope angles will have disastrous consequences for landslide susceptibility zonation.

The smoothening effect in InSAR DEM also limits the visual interpretation in 3-D perspective, e.g. using the anaglyph method, as the topographic details are blurred. As it has been observed in the profile, the smoothening effects are pronounced along the mountain tops and in the valleys. These are also the areas of low coherence due to layover and shadow. These low coherence areas are masked out before phase unwrapping (a coherence threshold is applied before unwrapping) and the phase values are interpolated and hence these are not the actual phase values. As a consequence, large height deviation compared with the reference DHM25, especially along the areas of high relief is noticed.

Acknowledgements

Part of this work was carried out in the framework of the DUP SLAM2 project "Service for Landslides Monitoring - Integration of Remote Sensing techniques with statistical methods for Landslide Monitoring and Risk Assessment" for the European Space Agency.

We would like to thank Olivier Lateltin and Hugo Raetzo of the Swiss Federal Office for Water and Geology (FOWG) for providing us the landslide map of the study area, and Swisstopo for providing us the DHM25 Digital Elevation Model.

REFERENCES

Balmer, R. (2003). http://www.ifp.uni-stuttgart.de/publications/phowo99/bamler.pdf

Bonham-Carter, G.F. (1994). Geographic Information Systems for Geoscientists. Modelling with GIS. *Computer Methods in the Geosciences*, Pergamon **13**, 267- 302.

Bulmer, M.H., Campbell, B. A., and Byrnes, J. (2001). Field studies and Radar remote sensing of silicic lawa flows. *Lunar and Planetary Science Conference*, XXXI, 18-50.

Chips (2002). http://www.geogr.ku.dk/chips/Manual/f167.htm

Crosetto, M. (2002). Calibration and validation of SAR interferometry for DEM generation. *ISPRS Journal of Photogrammetry and Remote Sensing*, **57,** 213-227.

De Grandi, G.F., Leysen, M., Lee, J.S., and Schuler, D. (1997). Radar reflective estimation using multiple SAR scenes of the same target: techniques and applications, *Proceedings of IGARRS conference*, Singapore, 1997, pp 1047-1050

Fruneau, B., Achache, J., and Delacourt, C. (1996). Observations and modeling of the Saint-Etiemme-de-Tinee landslide using SAR interferometry. *Tectonophysics,* **265**, 181-190.

Gens, R. and van Genderen, J. L. (1996). SAR Interferometry – Issues, Techniques, Applications. *International Journal of Remote Sensing*, **17**, 1803-1835.

Holecz, F., Pasquali, P., Moreira, J., Meier, E. and Nüesch, D. (1998). Automatic Generation and Quality Assessment of Digital Surface Models generated from AeS-1 InSAR data. *Proceedings of European Conference on Synthetic Aperture Radar,* Friedrichshafen, Germany.

Monbaron, M., Stoffel, M. and Gartner, H. (2002). http://www.unifr.ch/geoscience/geographie/Research/PHYSICAL/GEOMORP/Dendro.htm

Pasquali, P. Pellegrini, R., Prati, C. and Rocca, F. (1994). Combination of interferograms from ascending and descending orbits. *International Geosciences and Remote Sensing Symposium.* Pasadena, CA, USA, 8-12 August, 1994. pp 733-735.

Platschorre, Y. (1997). *A quantitative analysis of space borne derived elevation models.* Unpublished M. Sc. thesis, Delft University of Technology, 97pp.

Reigber A. and Moreira, J. (1997). Phase unwrapping by fusion of local and global methods. *Proceedings of IGARSS Symposium*, Singapore. (INCLUDE PAGES)

Rott H., Scheuchl, B., Siegel, A., and Grasemann, B. (1999). Monitoring very slow slope movements by means of SAR interferometry: a case study from a mass waste above a reservoir in the Ötztal Alps, Austria. *Geophysical Research Letters*, **26**, 1629-1632.

Sarmap (2002). http://www.sarmap.ch/

Swisstopo (2002). http://www.swisstopo.ch/en/digital/dhm25.htm
Van Westen, C.J. (1993) Application of Geographic Information Systems to Landslide Hazard Zonation. PhD Dissertation Technical University Delft. ITC Publication no. 15a, ITC, Enschede, the Netherlands, 245 pp.
Vietmeier J., Wagner, W. and Dikau, R. (1999). Monitoring moderate slope movements (landslides) in the southern French Alps using differential SAR interferometry, Fringes 99.